25. Ronzoni M, Manzoni M, Mariucci S, Loupakis F, Brugnatelli S, Bencardino K, et al. Circulating endothelial cells and endothelial progenitors as predictive markers of clinical response to bevacizumab-based first-line treatment in advanced colorectal cancer patients. *Ann Oncol.* 2010;21:2382–9.
26. Allard WJ, Matera J, Miller MC, Repollet M, Connelly MC, Rao C, et al. Tumor cells circulate in the peripheral blood of all major carcinomas but not in healthy or patients with nonmalignant diseases. *Clin Cancer Res.* 2004;10:6897–904.
27. Tanaka F, Yoneda K, Kondo N, Hashimoto M, Takuwa T, Matsumoto S, et al. Circulating tumor cell as a diagnostic marker in primary lung cancer. *Clin Cancer Res.* 2009;15:6980–6.
28. Alix-Panabières, C, Riethdorf S, Pantel K. Circulating tumor cells and bone marrow micrometastasis. *Clin Cancer Res.* 2008;14: 5013–21.
29. Curren D, Sahmound T, Therasse P, van Meerbeeck J, Postmus PE, Giaccone G. Prognostic factors in patients with pleural mesothelioma: the European Organization for Research and Treatment of cancer experience. *J Clin Oncol.* 1998;16:145–52.
30. Fennell DA, Parmer A, Shamash J, Evans MT, Sheaff MT, Sylvester R, et al. Statistical validation of the EORTC prognostic model for malignant pleural mesothelioma based on three consecutive phase II studies. *J Clin Oncol.* 2005;23:184–9.

Cellular Physiology and Biochemistry

Cell Physiol Biochem 2012;30:61-74
DOI: 10.1159/000339048
Published online: June 08, 2012
Accepted: May 02, 2012

1015-8987/12/0301-0061$38.00/0

Original Paper

AMP Converted from Intracellularly Transported Adenosine Upregulates p53 Expression to Induce Malignant Pleural Mesothelioma Cell Apoptosis

Yoshitaka Nogi[1,2*] Takeshi Kanno[1*] Takashi Nakano[2,3] Yumiko Fujita[1,2] Chiharu Tabata[2] Kazuya Fukuoka[3] Akinobu Gotoh[4] Tomoyuki Nishizaki[1]

[1]Division of Bioinformation, Department of Physiology, Hyogo College of Medicine, Nishinomiya, [2]Division of Pulmonary Medicine, Department of Internal Medicine, Hyogo College of Medicine, Nishinomiya, [3]Cancer Center, Hyogo College of Medicine, Nishinomiya, [4]Laboratory of Cell and Gene Therapy, Institute for Advanced Medical Sciences, Hyogo College of Medicine, Nishinomiya, *Y. Nogi and T. Kanno contributed equally to this work

Key Words
Adenosine • AMP • p53 • Malignant pleural mesothelioma cell • Apoptosis

Abstract
Background/Aims: The present study investigated adenosine-induced apoptosis in human malignant pleural mesothelioma cells. ***Methods:*** MTT assay, TUNEL staining, flow cytometry using propidium iodide and annexin V-FITC, real-time RT-PCR, Western blotting, and assay of caspase-3, -8, and -9 activities were carried out using malignant pleural mesothelioma cell lines such as NCI-H28, NCI-H2052, NCI-H2452, and MSTO-211H cells, and p53 or A_3 adenosine receptor was knocked-down by transfecting each siRNA into cells. ***Results:*** Adenosine induced apoptosis in all the malignant pleural mesothelioma cells used here, independently of caspase activation. The adenosine effect was prevented by the adenosine transporter inhibitor dipyridamole, the adenosine kinase inhibitor ABT-702, or the A_3 adenosine receptor inhibitor MRS1191. Adenosine upregulated expression of the p53 mRNA and protein, that is abolished by ABT-702, but not by knocking-down A_3 adenosine receptor. Adenosine-induced apoptosis in NCI-H28 cells was significantly inhibited by knocking-down p53 and in part by knocking-down A_3 adenosine receptor. ***Conclusion:*** The results of the present study show that AMP converted from intracellularly transported adenosine upregulates p53 expression to induce caspase-independent apoptosis in malignant pleural mesothelioma cells and that A_3 adenosine receptor also participates partially in the apoptosis by the different mechanism.

Introduction

Malignant pleural mesothelioma, a highly aggressive neoplasm, has been increasing in incidence and is strongly associated with asbestos exposure [1]. Malignant pleural

Prof. Tomoyuki Nishizaki

Division of Bioinformation, Department of Physiology, Hyogo College of Medicine
1-1 Mukogawa-cho, Nishinomiya 663-8501 (Japan)
Tel. +81-798-45-6397, Fax +81-798-45-6649
E-mail: tomoyuki@hyo-med.ac.jp

mesothelioma is characterized by insidious growth and clinical presentation at an advanced stage of disease. In spite of extensive and intensive challenges, the treatment of malignant pleural mesothelioma has been still limited to marginally effective chemotherapy and morbid surgery.

Higher concentrations of extracellular adenosine are recognized to induce apoptosis in a variety of cancer cells via diverse signaling pathways. The underlying pathways are largely divided into two pathways, i.e., intrinsic and extrinsic pathways. For the intrinsic pathway, the initial step is uptake of extracellular adenosine into cells through adenosine transporters. Intracellularly transported adenosine is converted to AMP by adenosine kinase and activate AMP-activated protein kinase (AMPK), thereby inducing apoptosis in GT3-TKB human lung cancer cells and HuH-7 human hepatoma cells [2, 3]. Intracellularly transported adenosine/converted AMP downregulates expression of c-Fas-associated death domain protein (FADD)-like interleukin-1β-converting enzyme inhibitory protein (c-FLIP) to neutralize caspase-8 inhibition due to c-FLIP, resulting in the activation of caspase-8 and the effector caspase-3, to induce HuH-7 cell apoptosis [4]. Intracellularly transported adenosine, alternatively, activates caspase-3 by neutralizing caspase-3 inhibition due to inhibitor of apoptosis protein (IAP) as a result of decreased IAP2 expression and reduced IAP activity in response to increased DIABLO expression and DIABLO release from damaged mitochondria in HuH-7 cells, regardless of caspase-9 activation [5]. Moreover, intracellularly transported adenosine induces caspase-independent apoptosis in MCF-7 human breast cancer cells by accumulating AMID in the nucleus [6] or adenosine induces HuH-7 cell apoptosis in a caspase-independent manner by upregulating expression of AMID [7]. Adenosine also upregulates expression of mRNAs for tumor necrosis factor (TNF), TNF receptor 1-associated death domain protein (TRADD), TNF-related apoptosis inducing ligand receptor 2 (TRAIL-R2), receptor-interacting protein kinase 1 (RIPK1), and FADD in HepG2 human hepatoma cells, which suggests that adenosine induces HepG2 cell apoptosis by activating caspase-8 through a TNFR1/TRADD/RIP1/FADD pathway and the effector caspases-3 [8].

For the extrinsic pathway, adenosine receptors such as A_1, A_{2a}, A_{2b}, and A_3 receptors mediate apoptosis. Adenosine induces apoptosis in CW2 human colonic cancer cells by activating caspase-3, -8, and -9 via A_1 adenosine receptor linked to G_i protein [9]. Adenosine induces RCR-1 astrocytoma cell apoptosis by activating caspase-3/-9 in part via A_1 adenosine receptor [10]. Adenosine induces apoptosis in Caco-2 human colonic cancer cells by activating caspase-9/-3 via A_{2a} adenosine receptor linked to G_s protein [11] or HepG2 cell apoptosis by downregulating Bcl-X_L expression and upregulating Bid expression, causing activation of caspase-9/-3, via A_{2a} adenosine receptor [12]. A_3 adenosine receptor, that is linked to G_i or G_q protein, mediates apoptosis in human lung cancer cells, hepatocellular carcinoma cells, thyroid cancer cells, and breast cancer cells [13-16]. A study shows that adenosine prevents malignant pleural mesothelioma cell growth via A_3 adenosine receptor [17]. Little, however, is known about adenosine-induced apoptosis in malignant pleural mesothelioma cells.

The present study was designed to explore adenosine-induced apoptosis in human malignant pleural mesothelioma cells and to understand the underlying mechanism. We show here that for a main pathway AMP converted from intracellularly transported adenosine upregulates expression of p53, to induce caspase-independent apoptosis in malignant pleural mesothelioma cells and that for a branch pathway A_3 adenosine receptor mediates the apoptosis by the different mechanism.

Materials and Methods

Cell culture

Human malignant pleural mesothelioma cell lines such as NCI-H28, NCI-H2052, NCI-H2452, and MSTO-211H cells, originated from the epithelium, were purchased from American Type Culture Collection (Manassas, VA, USA). Cells were grown in RPMI-1640 medium supplemented with 10% heat-inactivated FBS, 0.003% L-glutamine, penicillin (final concentration, 100 U/ml), and streptomycin (final concentration, 0.1 mg/ml), in a humidified atmosphere of 5% CO_2 and 95% air at 37 °C.

Cellular Physiology and Biochemistry

Cell Physiol Biochem 2012;30:61-74
DOI: 10.1159/000339048
Published online: June 08, 2012

Table 1. Primers used for real-time RT-PCR

PCR primers	Oligonucleotide sequence
AIF	Sense: 5′-CACAAAGACACTGCGATTCAAACAGT-3′ Anti-sense: 5′-GTTGCTGAGGTATTCGGGGAGGAT-3′
AMID	Sense: 5′-GGGTTCGCCAAAAAGACATTCATTT-3′ Anti-sense: 5′-CCTCTGTGCCTTTGTCCGTCTGC-3′
p53	Sense: 5′-GCCATCTACAAGCAGTCACAGCACAT-3′ Anti-sense: 5′-GGCACAAACACGCACCTCAAAGC-3′
GAPDH	Sense: 5′-GACTTCAACAGCGACACCCACTCC-3′ Anti-sense: 5′-AGGTCCACCACCCTGTTGCTGTAG-3′

Assay of cell viability

Cell viability was evaluated by the method using 3-(4,5-dimethyl-2-thiazolyl)-2,5-diphenyl-2H-tetrazolium bromide (MTT) as previously described [2].

Terminal deoxynucleotidyl transferase-mediated dUTP nick end labeling (TUNEL) staining

TUNEL staining was performed to detect in situ DNA fragmentation as a marker of apoptosis using an In Situ Apoptosis Detection Kit (Takara Bio, Otsu, Japan). Briefly, fixed and permeabilized cells were reacted with terminal deoxynucleotidyl transferase and fluorescein isothiocyanate (FITC)-deoxyuridine triphosphate for 90 min at 37 °C. FITC signals were visualized with a confocal scanning laser microscope (LSM 510, Carl Zeiss Co., Ltd., Oberkochen, Germany).

Apoptosis assay

Cells were suspended in a binding buffer before and after treatment with adenosine and stained with both propidium iodide (PI) and annexin V-FITC, and loaded on a flow cytometer (FACSCalibur, Becton Dickinson, Franklin Lakes, USA) available for FL1 (annexin V) and FL2 (PI) bivariate analyisis. Data from 10,000 cells/sample were collected, and the quadrants were set according to the population of viable, unstained cells in untreated samples. CellQuest analysis of the data was used to calculate the percentage of the cells in the respective quadrants.

Real-time reverse transcription-polymerase chain reaction (RT-PCR)

Total RNAs of cells were purified by an acid/guanidine/thiocyanate/chloroform extraction method using the Sepasol-RNA I Super kit (Nacalai, Kyoto, Japan). After purification, total RNAs were treated with RNase-free DNase I (2 units) at 37 °C for 30 min to remove genomic DNAs, and 10 μg of RNAs was resuspended in water. Then, random primers, dNTP, 10x RT buffer, and Multiscribe Reverse Transcriptase were added to an RNA solution and incubated at 25 °C for 10 min followed by 37 °C for 120 min to synthesize the first-strand cDNA. Real-time RT-PCR was performed using a SYBR Green Realtime PCR Master Mix (Takara Bio) and the Applied Biosystems 7900 real-time PCR detection system (ABI, Foster City, CA, USA). Thermal cycling conditions were as follows: first step, 94 °C for 4 min; the ensuing 40 cycles, 94 °C for 1 s, 65 °C for 15 s, and 72 °C for 30 s. The expression level of each mRNA was normalized by that of GAPDH mRNA. Primers used for real-time RT-PCR are shown in Table 1.

Construction and transfection of siRNA

The siRNA to silence human p53-targeted gene (p53 siRNA) was obtained from Santa Cruz Biotechnology (Santa Cruz, CA, USA), the siRNA to silence GATA-2-targeted gene (GATA-2 siRNA) from Cosmo Bio Co. Ltd. (Tokyo, Japan), and the siRNA to silence the A_3 adenosine receptor-targeted gene (A_3R siRNA) and the negative control siRNA (NC siRNA) from Ambion (Austin, TX, USA).

The p53 siRNA, the GATA-2 siRNA, the A_3R siRNA, or the NC siRNA was reverse-transfected into cells using a Lipofectamine reagent (Invitrogen, Carlsbad, CA, USA). Cells were used for experiments 48 h after transfection.

Separation into the nuclear and cytosolic components

Cells were suspended in buffer A [25 mM $MgCl_2$, 0.1 % (v/v) Triton X-100, 1 mM dithiothreitol, and 10 mM HEPES, pH 7.6] containing 1% (v/v) protease inhibitor cocktail, and then centrifuged at 3,500 rpm for 5 min at 4 °C. The pellet and supernatant were used as nuclei- and cytosol-enriched components. Whether

Cell Physiol Biochem 2012;30:61-74
DOI: 10.1159/000339048
Published online: June 08, 2012

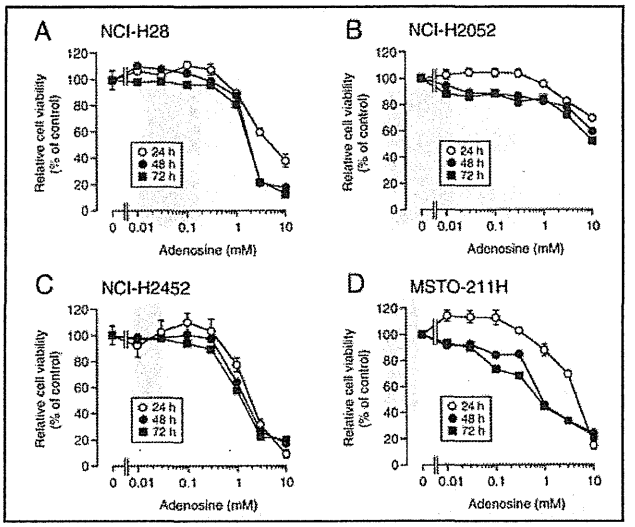

Fig. 1. Cell viability. NCI-H28 (A), NCI-H2052 (B), NCI-H2452 (C), and MSTO-211H cells (D) were treated with adenosine at concentrations as indicated for 24-72 h, and cell viability was quantified with an MTT assay. In the graphs, each point represents the mean (± SEM) percentage of control (MTT intensities of cells untreated with adenosine)(n=4 independent experiments).

the nuclear and cytosolic components were successfully separated was confirmed by Western blotting using an anti-Lamin A/C antibody, a nuclear marker.

Western blotting

Cells were lysed with 1% (w/v) sodium dodecyl sulfate (SDS). Proteins were separated by SDS-polyacrylamide gel electrophoresis (SDS-PAGE) using a TGX gel (BioRad, Hercules, CA, USA) and then transferred to polyvinylidene difluoride membranes. Blotting membranes were blocked with TBS-T [150 mM NaCl, 0.1% (v/v) Tween20 and 20 mM Tris, pH 7.5] containing 5% (w/v) bovine serum albumin and subsequently incubated with an anti-AIF antibody (Santa Cruz Biotechnology), an anti-AMID antibody (Santa Cruz Biotechnology), an anti-p53 antibody (Cell Signaling, Beverly, MA, USA), an anti-GATA-2 antibody (Santa Cruz Biotechnology), an anti-A_3 receptor antibody (Santa Cruz Biotechnology), or an anti-β-actin antibody (Sigma, St Louis, MO, USA). After washing, membranes were reacted with a horseradish peroxidase-conjugated goat anti-mouse IgG or goat anti-rabbit IgG antibody. Immunoreactivity was detected with an ECL kit (GE Healthcare, Piscataway, NJ, USA) and visualized using a chemiluminescence detection system (GE Healthcare). Protein concentrations for each sample were determined with a BCA protein assay kit (Pierce, Rockford, IL, USA).

Enzymatic assay of caspase-3, -8, and -9 activities

Caspase activity was measured using a caspase fluorometric assay kit (Ac-Asp-Glu-Val-Asp-MCA for a caspase-3 substrate peptide; Ac-Ile-Glu-Thr-Asp-MCA for a caspase-8 substrate peptide; and Ac-Leu-Glu-His-Asp-MCA for a caspase-9 substrate peptide) as previously described [11]. Briefly, NCI-H28 cells were harvested before and after treatment with adenosine, and then centrifuged at 1,200 rpm for 5 min at 4 °C. The pellet was incubated on ice in cell lysis buffer for 10 min, and reacted with the fluorescently labeled tetrapeptide at 37 °C for 2 h. The fluorescence was measured at an excitation of wavelength of 380 nm and an emission wavelength of 460 nm with a fluorometer (Fluorescence Spectrometer, F-4500, HITACHI, Japan).

Statistical analysis

Statistical analysis was carried out using unpaired *t*-test and Dunnett's test.

Results

Extracellular adenosine induces apoptosis in malignant pleural mesothelioma cells via both the extrinsic and intrinsic pathways

In the MTT assay, extracellular adenosine reduced cell viability for all the malignant pleural mesothelioma cells used here such as NCI-H28, NCI-H2052, NCI-H2452, and MSTO-211H cells in a concentration (0.01-10 mM)- and treatment time (24-72h)-dependent

Cell Physiol Biochem 2012;30:61-74
DOI: 10.1159/000339048
Published online: June 08, 2012

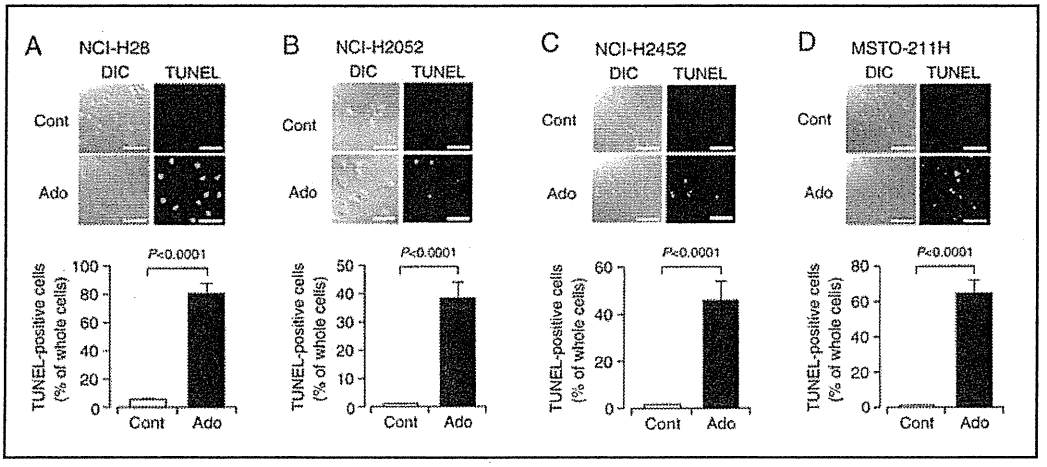

Fig. 2. TUNEL staining. TUNEL staining was carried out in NCI-H28 (A), NCI-H2052 (B), NCI-H2452 (C), and MSTO-211H cells (D) untreated (Cont) and treated with adenosine (Ado)(3 mM) for 24 h. DIC, differential interference contrast. Bars, 100 μm. TUNEL-positive cells were counted in the area (0.4 mm x 0.4 mm) selected at random. In the graphs, each column represents the mean (± SEM) TUNEL-positive cell percentage of whole cells (n=4 independent experiments). *P* values, unpaired *t*-test.

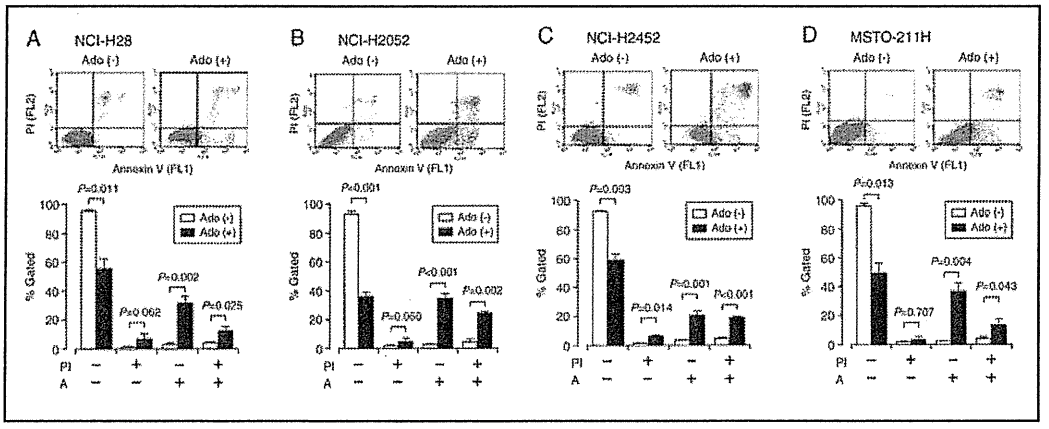

Fig. 3. Flow cytometry. NCI-H28 (A), NCI-H2052 (B), NCI-H2452 (C), and MSTO-211H cells (D) were untreated [Ado (-)] and treated with adenosine (3 mM) for 24 h [Ado (+)], and then flow cytometry using PI and annexin V-FITC was carried out. Typical profiles are shown in the upper panels. In the graphs, each column represents the mean (± SEM) percentage of cells in 4 fractions against total cells (n=4 independent experiments). *P* values, Dunnett's test.

manner, with the order of the potential for: NCI-H2452 cells>NCI-H28 cells>MSTO-211H cells>NCI-H2052 cells (Fig. 1A,B,C,D). This indicates that adenosine induces cell death in malignant pleural mesothelioma cells, although the potential varies depending upon the cell types.

To see whether the adenosine-induced cell death is due to necrosis or apoptosis, we carried out TUNEL staining. Treatment with adenosine (3 mM) for 24 h significantly increased the number of TUNEL-positive cells as compared with that before adenosine treatment commonly for all the malignant pleural mesothelioma cells examined here with the degree varying among cell types (Fig. 2A,B,C,D). This indicates that adenosine induces apoptosis in malignant pleural mesothelioma cells.

To obtain further evidence for adenosine-induced apoptosis, we carried out flow cytometry using PI and annexin V-FITC. PI is a marker of dead cells and annexin V, detecting

Cell Physiol Biochem 2012;30:61-74
DOI: 10.1159/000339048
Published online: June 08, 2012

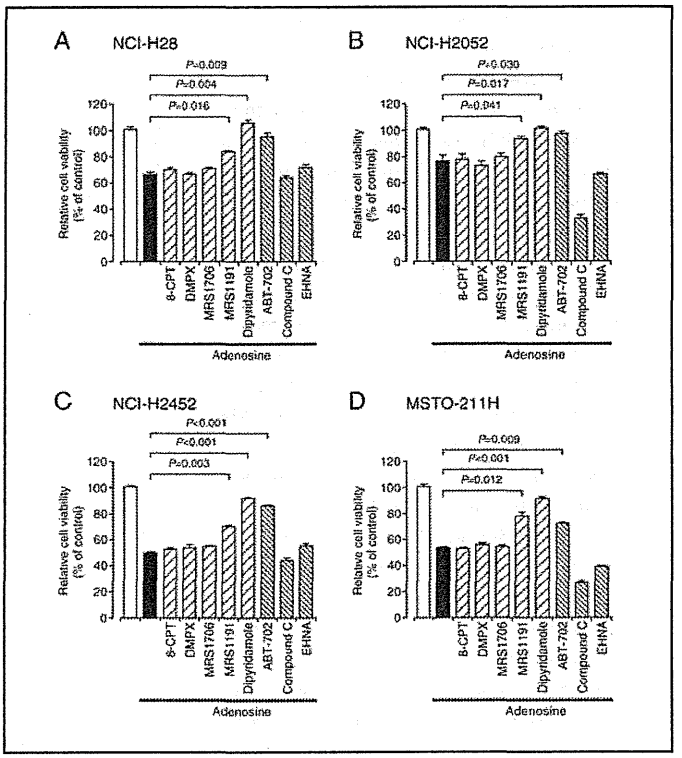

Fig. 4. Pharmacological analysis using inhibitors. NCI-H28 (A), NCI-H2052 (B), NCI-H2452 (C), and MSTO-211H cells (D) were treated with adenosine (3 mM) in the absence and presence of 8-CPT (10 μM), DMPX (10 μM), MRS1706 (50 nM), MRS1191 (10 μM), dipyridamole (10 μM), ABT-702 (1 μM), Compound C (10 μM), or EHNA (10 μM) for 24 h, and then, MTT assay was carried out. In the graphs, each column represents the mean (± SEM) percentage of basal levels (MTT intensities of cells untreated with adenosine in the absence of inhibitors)(n=4 independent experiments). *P* values, Dunnett's test.

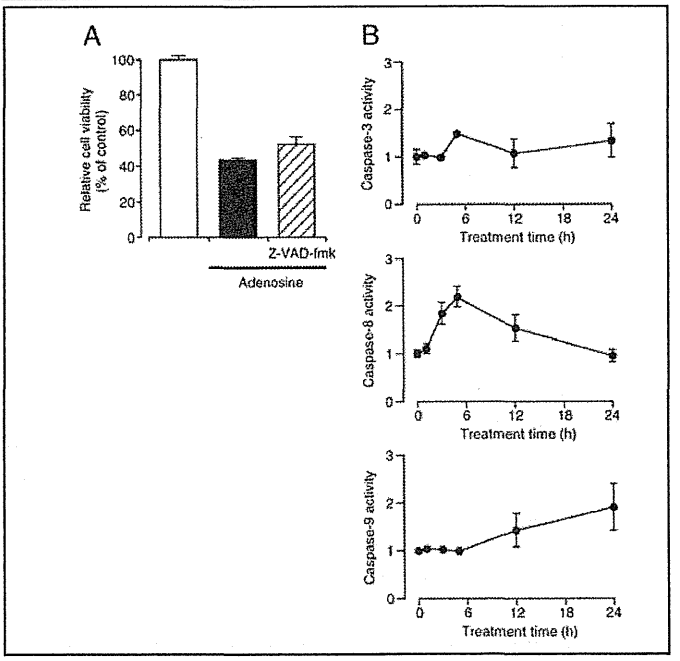

Fig. 5. Caspase activity. (A) NCI-H28 cells were treated with adenosine (3 mM) in the presence and absence of Z-VAD-fmk (100 μM) for 24 h, followed by MTT assay. In the graph, each column represents the mean (± SEM) percentage of control (MTT intensities of cells untreated with adenosine in the absence of the Z-VAD-fmk)(n=4 independent experiments). (B) NCI-H28 cells were treated with adenosine (3 mM) for 1-24 h, and then activities of caspase-3, -8, and -9 were enzymatically assayed. In the graphs, each point represents the mean (± SEM) ratio against basal caspase activities (before treatment with adenosine)(n=4 independent experiments).

externalized phosphatidylserine residues, is a marker of apoptotic cells [18]. For all the cell types, 24-h treatment with adenosine (3 mM) markedly decreased the population of PI-negative and annexin V-negative cells, but otherwise it significantly increased the population of PI-negative and annexin V-positive cells and the population of PI-positive and annexin V-positive cells, each corresponding to early apoptosis and late apoptosis/secondary necrosis [19](Fig. 3A,B,C,D). Collectively, these results provide evidence for adenosine-induced apoptosis in malignant pleural mesothelioma cells.

For all the malignant pleural mesothelioma cells used here, adenosine-induced cell death was significantly inhibited by 3-ethyl 5-benzyl-2- methyl-6-phenyl-4-phenylethynyl-

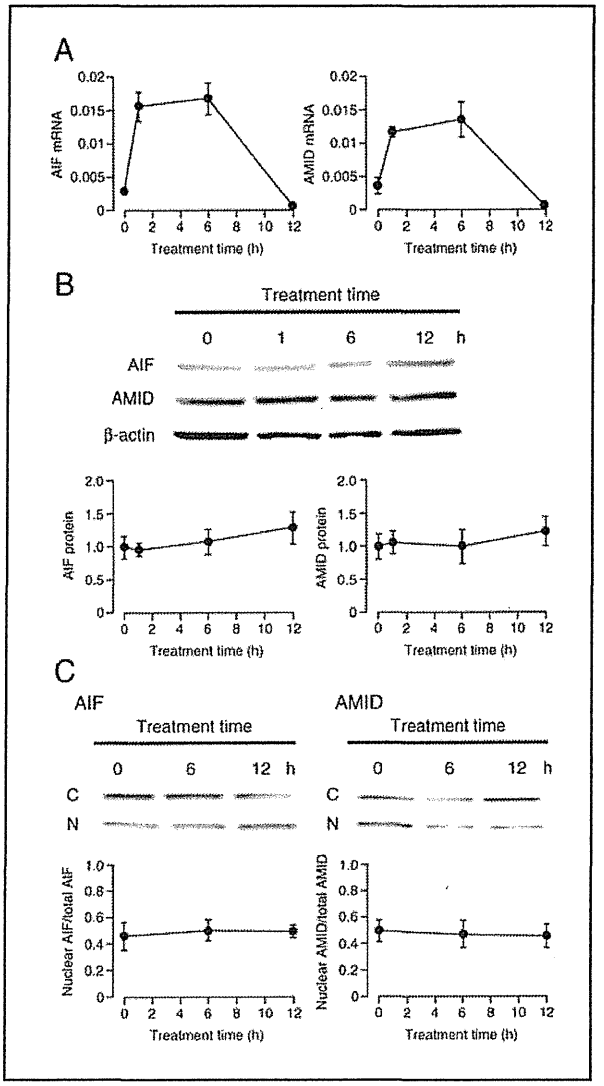

Fig. 6. Expression and intracellular distribution of AIF and AMID. (A) NCI-H28 cells were treated with adenosine (3 mM) for periods of time as indicated, and then real-time RT-PCR was carried out. Signal intensities for the AIF and AMID mRNAs were normalized by the intensity for the GAPDH mRNA. In the graphs, each point represents the mean (± SEM) normalized AIF or AMID mRNA intensity (n=4 independent experiments). (B) NCI-H28 cells were treated with adenosine (3 mM) for periods of time as indicated, and then Western blotting was carried out. Signal intensities for AIF or AMID protein were normalized by the intensity for β-actin. In the graphs, each point represents the mean (± SEM) ratio against signal intensities for AIF or AMID protein at 0 h (n=4 independent experiments). (C) NCI-H28 cells treated with adenosine (3 mM) for periods of time as indicated were lysed and separated into the nuclear (*N*) and cytosolic components (*C*), followed by Western blotting. In the graphs, each point represents the mean (± SEM) ratio: nuclear AIF or AMID/whole cell AIF or AMID (n=4 independent experiments).

1,4-(±)-dihydropyridine-3,5-dicarboxylate (MRS1191), an inhibitor of A_3 adenosine receptors, while it was not affected by 8-cyclopentyltheophylline (8-CPT), an inhibitor of A_1 adenosine receptors, 3,7-dimethyl-1 propargylxanthine (DMPX), an inhibitor of A_{2a} adenosine receptors, or *N*-(4-acetylphenyl)-2-[4-(2,3,6,7-tetrahydro-2,6-dioxo-1,3-dipropyl-1*H*-purin-8-yl)phenoxy]acetamide (MRS1706), an inhibitor of A_{2b} adenosine receptors (Fig. 4A,B,C,D). This indicates that A_3 adenosine receptor participates in malignant pleural mesothelioma cell death, i.e., adenosine induces apoptosis in malignant pleural mesothelioma cells through an extrinsic pathway.

Adenosine-induced cell death for malignant pleural mesothelioma cells, alternatively, was neutralized by dipyridamole, an adenosine transporter inhibitor (Fig. 4A,B,C,D), indicating the participation of intrinsic pathway too in adenosine-induced malignant pleural mesothelioma cell death. The adenosine-induced cell death was also significantly suppressed by 4-amino-5-(3-bromophenyl)-7-(6-morpholino-pyridin-3-yl)pyrido[2,3-d] pyrimidine (ABT-702), an inhibitor of adenosine kinase to phosphorylate adenosine and convert to AMP, but it was not affected by Compound C, an inhibitor of AMPK (Fig. 4A,B,C,D). This interprets that AMP converted from intracellularly transported adenosine mediates adenosine-induced apoptosis in malignant pleural mesothelioma cells, without AMPK activation. Moreover, the adenosine-induced cell death was not inhibited by erythro-9-(2-hydroxy-3-nonyl) adenine

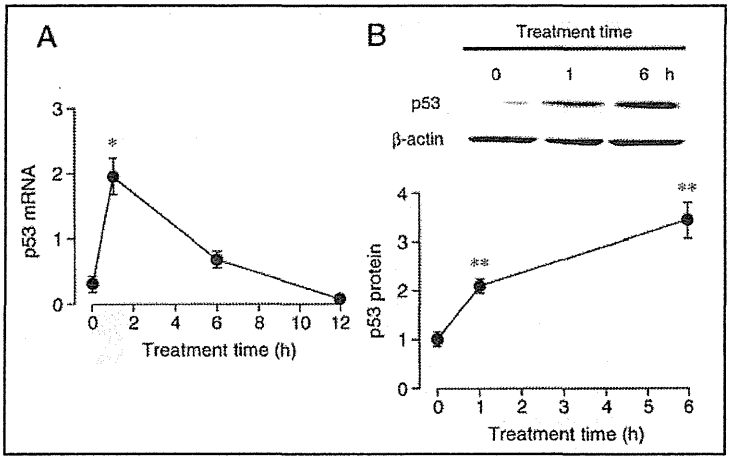

Fig. 7. p53 expression. NCI-H28 cells were treated with adenosine (3 mM) for periods of time as indicated, followed by real-time RT-PCR (A) and Western blotting (B). (A) Signal intensities for the p53 mRNA was normalized by the intensity for the GAPDH mRNA. In the graph, each point represents the mean (± SEM) normalized p53 mRNA intensity (n=4 independent experiments). *P<0.01 as compared with basal levels (0 h), Dunnett's test. (B) Signal intensities for p53 protein were normalized by the intensity for β-actin. In the graph, each point represents the mean (± SEM) ratio against p53 signal intensities at 0 h (n=4 independent experiments). **P<0.001 as compared with basal levels (0 h), Dunnett's test.

(EHNA), an inhibitor of adenosine deaminase (Fig. 4A,B,C,D), indicating that the adenosine effect is not caused by adenosine metabolites such as hypoxanthine and inosine.

Adenosine-induced apoptosis in NCI-H28 cells is largely independent of caspase activation

We next attempted to understand the intracellular signaling underlying adenosine-induced apoptosis in malignant pleural mesothelioma cells. To address this question, we picked up NCI-H28 cells with a moderate adenosine effect among 4 cell lines and used them for the following experiments.

Adenosine-induced NCI-H28 cell death was little inhibited by the pan-caspase inhibitor Z-VAD-fmk (Fig. 5A), suggesting caspase-independent apoptosis.

To further clarify this, we enzymatically assayed activities of caspase-3, -8, and -9. No apparent activation of caspase-3, -8, or -9 in NCI-H28 cells was obtained with adenosine (Fig. 5B), supporting the note that adenosine induces apoptosis in NCI-H28 cells largely in a caspase-independent manner.

In our earlier study, adenosine induces caspase-independent apoptosis in HuH-7 human hepatoma cells by upregulating AMID [7]. For a caspase-independent apoptotic pathway, AMID as well as AIF are the major executioners. AIF, that is localized within the mitochondrial membrane under the normal conditions, is released from the mitochondria in response to lethal signals, translocated into the nucleus, and binds to the nuclear DNA, thereby causing chromosomal condensation, margination, and large-scale DNA fragmentation [20-22]. Likewise, AMID induces apoptosis by accumulating in the nucleus [23-28]. In the present study, adenosine increased expression of mRNAs for AIF and AMID in a bell-shaped treatment time (1-12 h)-dependent manner in NCI-H28 cells (Fig. 6A). Strangely, adenosine did not alter expression of proteins for AIF and AMID in NCI-H28 cells (Fig. 6B). Additionally, no translocation of AIF or AMID from the cytosol into the nucleus was found with adenosine (Fig. 6C). Overall, these results indicate that adenosine induces caspase-independent apoptosis in NCI-H28 cells, regardless of AIF or AMID.

Adenosine induces NCI-H28 cell apoptosis in a p53-dependent manner

The tumor suppressor protein p53 is well-recognized to induce cancer cell apoptosis via transcription-dependent and -independent pathways. Then, our final attempt was to see whether p53 is implicated in adenosine-induced apoptosis here. For NCI-H28 cells, adenosine increased expression of the p53 mRNA in a bell-shaped treatment time (1-12 h)-dependent manner (Fig. 7A) and p53 protein in a treatment time (1-6 h)-dependent manner (Fig. 7B). This accounts for adenosine-induced upregulation of p53 expression in NCI-H28 cells.

Cell Physiol Biochem 2012;30:61-74
DOI: 10.1159/000339048
Published online: June 08, 2012

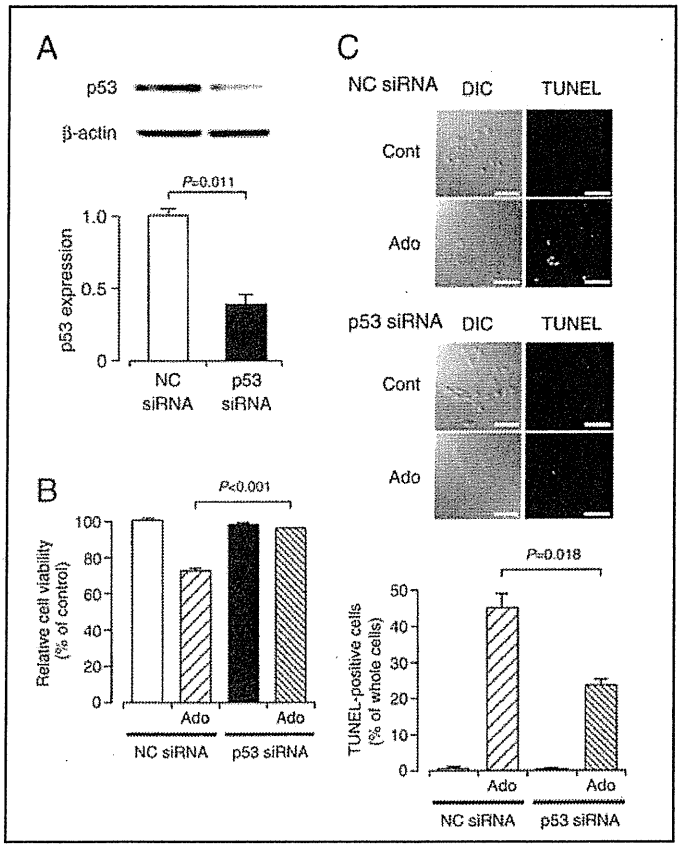

Fig. 8. p53-dependent apoptosis. (A) NCI-H28 cells were transfected with the NC siRNA or the p53 siRNA, and Western blotting was carried out 48 h after transfection. The signal intensity for p53 protein was normalized by the intensity for β-actin. In the graph, each column represents the mean (± SEM) ratio against p53 protein signal intensities for cells transfected with the NC siRNA (n=4 independent experiments). *P* value, unpaired *t*-test. (B) NCI-H28 cell viability was assayed in cells transfected with the NC siRNA or the p53 siRNA before and after 24-h treatment with adenosine (Ado)(3 mM). In the graph, each column represents the mean (± SEM) percentage of basal levels (MTT intensities of cells untreated with adenosine)(n=4 independent experiments). *P* value, Dunnett's test. (C) TUNEL staining was carried out in NCI-H28 cells transfected with the NC siRNA or the p53 siRNA before (Cont) and after 24-h treatment with adenosine (Ado)(3 mM). DIC, differential interference contrast. Bars, 100 μm. TUNEL-positive cells were counted in the area (0.4 mm x 0.4 mm) selected at random. In the graph, each column represents the mean (± SEM) TUNEL-positive cell percentage of whole cells (n=4 independent experiments). *P* value, Dunnett's test.

Expression of p53 protein for NCI-H28 cells transfected with the p53 siRNA was significantly attenuated as compared with the expression for cells transfected with the NC siRNA (Fig. 8A), confirming p53 knock-down. Adenosine-induced NCI-H28 cell death was significantly prevented by knocking-down p53 (Fig. 8B). In addition, adenosine-induced increase in TUNEL-positive cells was also significantly suppressed by knocking-down p53 (Fig. 8C). Taken together, these results indicate that adenosine induces NCI-H28 cell apoptosis by upregulating p53 expression.

We have earlier found that adenosine upregulates p53 expression by targeting GATA-2, thereby activating caspase-3, -8, and -9 to induce HepG2 cell apoptosis [29]. To see whether adenosine-induced upregulation of p53 expression in NCI-H28 cells is regulated by GATA-2, the GATA-2 siRNA was transfected into cells. Expression of GATA-2 protein for NCI-H28 cells transfected with the GATA-2 siRNA was significantly reduced as compared with the expression for cells transfected with the NC siRNA (Fig. 9A), confirming GATA-2 knock-down. Adenosine-induced upregulation of p53 mRNA expression in NCI-H28 cells was not affected by knocking-down GATA-2 (Fig. 9B). This indicates that adenosine promotes the p53 transcription in NCI-H28 cells in a GATA-2-independent manner.

For NCI-H28 cells transfected with the A_3R siRNA, expression of A_3 adenosine receptor protein was significantly suppressed as compared with the expression for cells transfected with the NC siRNA (Fig. 9C), confirming A_3 adenosine receptor knock-down. Adenosine-induced upregulation of p53 mRNA expression in NCI-H28 cells was not influenced by knocking-down A_3 adenosine receptor (Fig. 9D). This indicates that A_3 adenosine receptor is not implicated in the upregulation of p53 expression for NCI-H28 cells.

Cell Physiol Biochem 2012;30:61-74
DOI: 10.1159/000339048
Published online: June 08, 2012

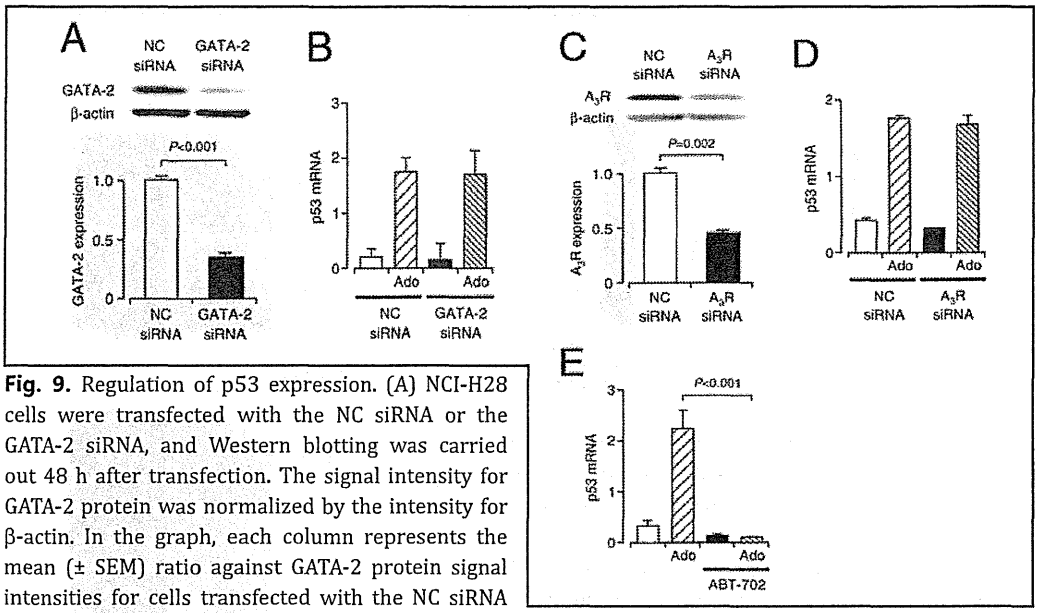

Fig. 9. Regulation of p53 expression. (A) NCI-H28 cells were transfected with the NC siRNA or the GATA-2 siRNA, and Western blotting was carried out 48 h after transfection. The signal intensity for GATA-2 protein was normalized by the intensity for β-actin. In the graph, each column represents the mean (± SEM) ratio against GATA-2 protein signal intensities for cells transfected with the NC siRNA (n=4 independent experiments). *P* value, unpaired *t*-test. (B) Real-time RT-PCR was carried out in cells transfected with the NC siRNA or the GATA-2 siRNA before and after 1-h treatment with adenosine (Ado)(3 mM). Signal intensities for the p53 mRNA was normalized by the intensity for the GAPDH mRNA. In the graph, each column represents the mean (± SEM) normalized p53 mRNA intensity (n=4 independent experiments). (C) NCI-H28 cells were transfected with the NC siRNA or the A_3R siRNA, and Western blotting was carried out 48 h after transfection. The signal intensity for A_3 adenosine receptor protein was normalized by the intensity for β-actin. In the graph, each column represents the mean (± SEM) ratio against A_3 adenosine receptor protein signal intensities for cells transfected with the NC siRNA (n=4 independent experiments). *P* value, unpaired *t*-test. (D) Real-time RT-PCR was carried out in cells transfected with the NC siRNA or the A_3R siRNA before and after 1-h treatment with adenosine (Ado)(3 mM). Signal intensities for the p53 mRNA was normalized by the intensity for the GAPDH mRNA. In the graph, each column represents the mean (± SEM) normalized p53 mRNA intensity (n=4 independent experiments). (E) Real-time RT-PCR was carried out in NCI-H28 cells before and after 1-h treatment with adenosine (Ado)(3 mM) in the presence and absence of ABT-702 (1 μM). Signal intensities for the p53 mRNA was normalized by the intensity for the GAPDH mRNA. In the graph, each column represents the mean (± SEM) normalized p53 mRNA intensity (n=4 independent experiments). *P* value, Dunnett's test.

Amazingly, adenosine-induced upregulation of p53 mRNA expression in NCI-H28 cells was drastically inhibited by the adenosine kinase inhibitor ABT-702 (Fig. 9E). This implies that AMP serves as a critical regulator for the p53 transcription.

Adenosine-induced reduction in NCI-H28 cell viability and adenosine-induced increase in TUNEL-positive cells was also inhibited by knocking-down A_3 adenosine receptor, but with a lesser degree as compared with that for knocking-down p53 (Fig. 10A,B). This suggests that A_3 adenosine receptor in part mediates NCI-H28 cell apoptosis by the mechanism distinct from AMP-mediated p53 upregulation.

Discussion

The results of the present study clearly demonstrate that extracellular adenosine induces apoptosis in malignant pleural mesothelioma cells such as NCI-H28, NCI-H2052, NCI-H2452, and MSTO-211H cells in a concentration (0.01-10 mM)- and treatment time (24-72h)-dependent manner, although the potential varies depending upon the cell types.

Accumulating evidence has shown that adenosine induces apoptosis in variety of cancer cells mainly through two pathways, i.e., an intrinsic pathway relevant to adenosine uptake

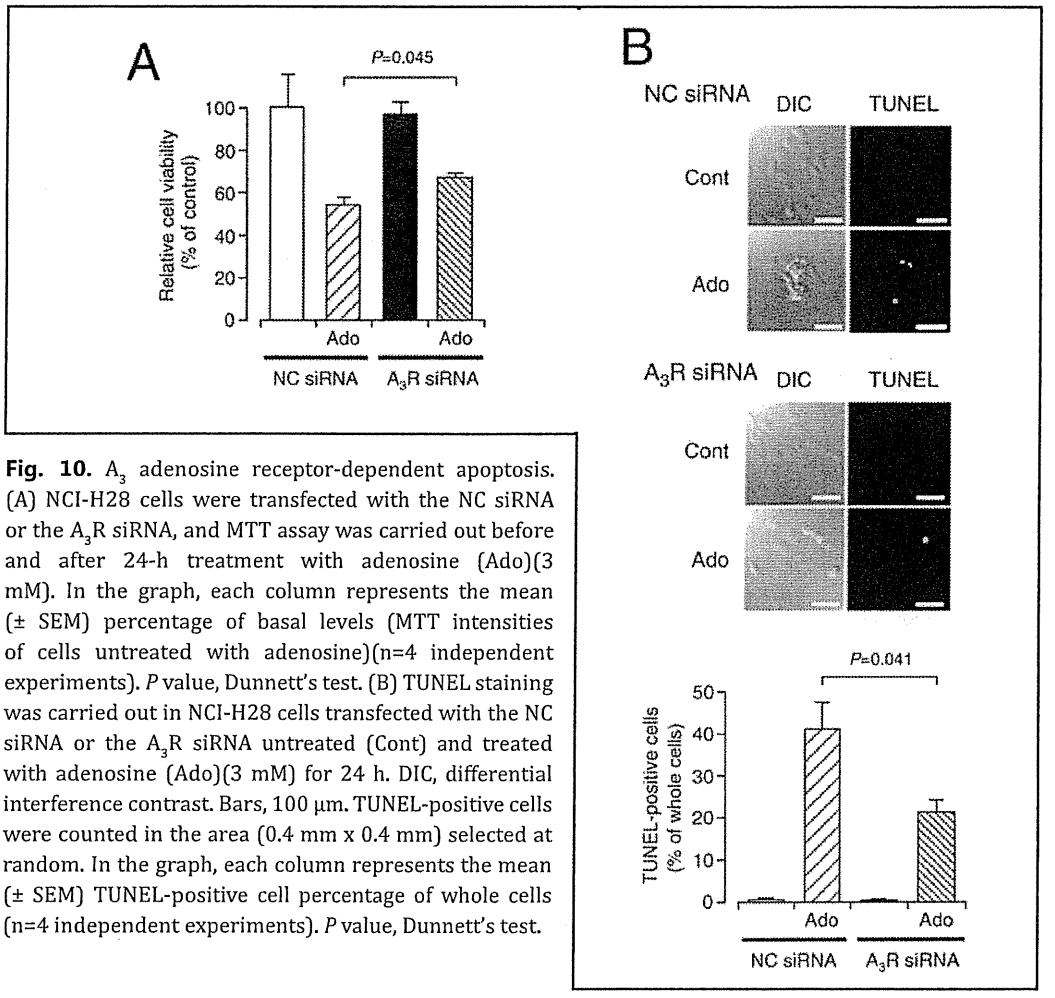

Fig. 10. A_3 adenosine receptor-dependent apoptosis. (A) NCI-H28 cells were transfected with the NC siRNA or the A_3R siRNA, and MTT assay was carried out before and after 24-h treatment with adenosine (Ado)(3 mM). In the graph, each column represents the mean (± SEM) percentage of basal levels (MTT intensities of cells untreated with adenosine)(n=4 independent experiments). *P* value, Dunnett's test. (B) TUNEL staining was carried out in NCI-H28 cells transfected with the NC siRNA or the A_3R siRNA untreated (Cont) and treated with adenosine (Ado)(3 mM) for 24 h. DIC, differential interference contrast. Bars, 100 μm. TUNEL-positive cells were counted in the area (0.4 mm x 0.4 mm) selected at random. In the graph, each column represents the mean (± SEM) TUNEL-positive cell percentage of whole cells (n=4 independent experiments). *P* value, Dunnett's test.

into cells and the ensuing signaling and an extrinsic pathway relevant to adenosine receptors that include A_1, A_{2a}, A_{2b}, and A_3 receptor. Adenosine-induced apoptosis in malignant pleural mesothelioma cells used here was almost reversed by the adenosine transporter inhibitor dipyridamole or the adenosine kinase inhibitor ABT-702. This interprets that extracellular adenosine induces apoptosis in malignant pleural mesothelioma cells via an intrinsic pathway, i.e., adenosine uptake into cells through adenosine transporters and ensuing conversion to AMP catalyzed by adenosine kinase. AMPK is shown to function downstream AMP, to induce apoptosis in GT3-TKB human lung cancer cells and HuH-7 human hepatoma cells [2, 3]. The adenosine effect here was not affected by the AMPK inhibitor Compound C. This suggests that AMPK is not a downstream target of AMP converted from intracellularly transported adenosine, responsible for adenosine-induced apoptosis in malignant pleural mesothelioma cells. Moreover, the adenosine effect was not inhibited by the adenosine deaminase inhibitor EHNA, indicating no participation of adenosine metabolites such as hypoxanthine and inosine in adenosine-induced malignant pleural mesothelioma cell apoptosis.

Adenosine-induced apoptosis in malignant pleural mesothelioma cells, alternatively, was significantly inhibited by the A_3 adenosine receptor inhibitor MRS1191, while the A_1 adenosine receptor inhibitor 8-CPT, the A_{2a} adenosine receptor inhibitor DMPX, or the A_{2b} adenosine receptor inhibitor MRS1706 had no effect. This indicates that extracellular adenosine also induces apoptosis in malignant pleural mesothelioma cells via an extrinsic pathway, i.e., via an A_3 adenosine receptor.

Two major pathways for apoptosis include caspase-dependent and -independent pathways. In the present study, adenosine-induced NCI-H28 cell death was not significantly

inhibited by the pan-caspase inhibitor Z-VAD-fmk. In addition, no remarkable activation of caspase-3, -8, and -9 was found with adenosine for NCI-H28 cells. Likewise, adenosine-induced cell death for the other cell lines NCI-H2052, NCI-H2452, and MSTO-211H cells was not significantly prevented by Z-VAD-fmk, and adenosine did not activate caspase-3, -8, and -9 in those cells (data not shown). Collectively, extracellular adenosine is likely to induce malignant pleural mesothelioma cell apoptosis mainly in a caspase-independent manner.

Then, one would ask the question how extracellular adenosine induces malignant pleural mesothelioma cell apoptosis. For a caspase-independent apoptotic pathway, AIF and AMID are recognized to serve as the major executioner. AIF and AMID induce apoptosis by accumulating in the nucleus [20-28]. We have earlier found that extracellular adenosine induces caspase-independent apoptosis in MCF-7 human breast cancer cells by accumulating AMID in the nucleus [6] or in HuH-7 cell apoptosis by upregulating expression of AMID [7]. In the present study, adenosine did not affect expression of proteins for AIF and AMID or intracellular distribution of AIF and AMID in NCI-H28 cells. This suggests no implication of AIF or AMID in adenosine-induced apoptosis in malignant pleural mesothelioma cells.

To explore the mechanism underlying adenosine-induced malignant pleural mesothelioma cell apoptosis, we highlighted p53, a tumor suppressor protein, bearing apoptosis in a wide variety of cancers. Amazingly, adenosine increased expression of the p53 mRNA and protein in NCI-H28 cells, and adenosine-induced NCI-H28 cell apoptosis was significantly prevented by knocking-down p53. Adenosine-induced upregulation of p53 expression and p53-dependent apoptosis were still obtained with the other cell lines NCI-H2052, NCI-H2452, and MSTO-211H cells (data not shown). These results raise the possibility that adenosine induces apoptosis in malignant pleural mesothelioma cells by upregulating p53 expression. In our earlier study, adenosine upregulated p53 expression under the control of GATA-2, responsible for adenosine-induced HepG2 cell apoptosis [29]. Adenosine-induced upregulation of p53 expression in NCI-H28 cells, however, was not affected by knocking-down GATA-2, indicating that adenosine here upregulates p53 expression, independently of GATA-2. Furthermore, the adenosine effect was not also inhibited by knocking-down A_3 adenosine receptor, indicating no mediation of the receptor in the p53 transcription for malignant pleural mesothelioma cells. The most striking finding in the present study is that adenosine-induced upregulation of p53 expression in NCI-H28 cells was completely inhibited by the adenosine kinase inhibitor ABT-702. This strongly suggests that AMP converted from intracellularly transported adenosine is engaged in the promotion of the p53 gene transcription. To our knowledge, this is the first suggesting AMP as a critical regulator for the p53 gene transcription.

Adenosine-induced apoptosis in NCI-H28 cells were still suppressed by knocking-down A_3 adenosine receptor, with the inhibition being lesser than that for knocking-down p53. This suggests that A_3 adenosine receptor in part mediates malignant pleural mesothelioma cell apoptosis by the mechanism independent of p53 upregulation.

In conclusion, the results of the present study show that for a main pathway extracellular adenosine is transported into cells and in turn, converted to AMP, which upregulates p53 expression to induce caspase-independent apoptosis in malignant pleural mesothelioma cells, and that for a branch pathway A_3 adenosine receptor participates in adenosine-induced apoptosis in malignant pleural mesothelioma cells. The results also suggest that AMP converted from intracellularly transported adenosine promotes the p53 gene transcription, responsible for malignant pleural mesothelioma cell apoptosis.

References

1 Raja S, Murthy SC, Mason DP: Malignant pleural mesothelioma. Curr Oncol Rep 2011;13:259-264.
2 Saitoh M, Nagai K, Nakagawa K, Yamamura T, Yamamoto S, Nishizaki T: Adenosine induces apoptosis in the human lung cancer cells via an intrinsic pathway relevant to activation of AMP-activated protein kinase. Biochem Pharmacol 2004;67:2005-2011.

3 Yang D, Yaguchi T, Nakano T, Nishizaki T: Adenosine activates AMPK to phosphorylate Bcl-X_L responsible for mitochondrial damage and DIABLO release in HuH-7 cells. Cell Physiol Biochem 2011;27:71-78.
4 Yang D, Yaguchi T, Yamamoto H, Nishizaki T: Intracellularly transported adenosine induces apoptosis in HuH-7 human hepatoma cells by downregulating c-FLIP expression causing caspase-3/-8 activation. Biochem Pharmacol 2007;73:1665-1675.
5 Yang D, Yaguchi T, Nakano T, Nishizaki T: Adenosine-induced caspase-3 activation by tuning Bcl-X_L/DIABLO/IAP expression in HuH-7 human hepatoma cells. Cell Biol Toxicol 2010;26:319-330.
6 Tsuchiya A, Kanno T, Saito M, Miyoshi Y, Gotoh A, Nakano T, Nishizaki T: Intracellularly transported adenosine induces MCF-7 human breast cancer cells by accumulating AMID in the nucleus. Cancer Lett 2012; in press.
7 Yang D, Yaguchi T, Nagata T, Gotoh A, Dovat S, Song C, Nishizaki T: AMID mediates adenosine-induced caspase-independent HuH-7 cell apoptosis. Cell Physiol Biochem 2011;27:37-44.
8 Yang D, Yaguchi T, Lim CR, Ishizawa Y, Nakano T, Nishizaki T: Tuning of apoptosis-mediator gene transcription in HepG2 human hepatoma cells through an adenosine signal. Cancer Lett 2010;291:225-229.
9 Saito M, Yaguchi T, Yasuda Y, Nakano T, Nishizaki T: Adenosine suppresses CW2 human colonic cancer growth by inducing apoptosis via A_1 adenosine receptors. Cancer Lett 2010;290:211-215.
10 Sai K, Yang D, Yamamoto H, Fujikawa H, Yamamoto S, Nagata T, Saito M, Yamamura T, Nishizaki T: A_1 adenosine receptor signal and AMPK involving caspase-9/-3 activation are responsible for adenosine-induced RCR-1 astrocytoma cell death. Neurotoxicol 2006;27:458-467.
11 Yasuda Y, Saito M, Yamamura T, Yaguchi T, Nishizaki T: Extracellular adenosine induces apoptosis in Caco-2 human colonic cancer cells by activating caspase-9/-3 via A_{2a} adenosine receptors. J Gastroenterol 2009;44:56-65.
12 Tamura K, Kanno T, Fujita Y, Gotoh A, Nakano T, Nishizaki T: A_{2a} adenosine receptor mediates HepG2 cell apoptosis by downregulating Bcl-X_L expression and upregulating Bid expression. J Cell Biochem 2012;doi: 10.1002/jcb.24048.
13 Bar-Yehuda S, Stemmer SM, Madi L, Castel D, Ochaion A, Cohen S, Barer F, Zabutti A, Perez-Liz G, Del Valle L, Fishman P: The A_3 adenosine receptor agonist CF102 induces apoptosis of hepatocellular carcinoma via de-regulation of the Wnt and NF-κB signal transduction pathways. Int J Oncol 2008;33:287-295.
14 Kim SJ, Min HY, Chung HJ, Park EJ, Hong JY, Kang YJ, Shin DH, Jeong LS, Lee SK: Inhibition of cell proliferation through cell cycle arrest and apoptosis by thio-Cl-IB-MECA, a novel A_3 adenosine receptor agonist, in human lung cancer cells. Cancer Lett 2008;264:309-315.
15 Morello S, Sorrentino R, Porta A, Forte G, Popolo A, Petrella A, Pinto A: Cl-IB-MECA enhances TRAIL-induced apoptosis via the modulation of NF-κB signalling pathway in thyroid cancer cells. J Cell Physiol 2009;221:378-386.
16 Panjehpour M, Karami-Tehrani F: Adenosine modulates cell growth in the human breast cancer cells via adenosine receptors. Oncol Res 2007;16:575-85.
17 Varani K, Maniero S, Vincenzi F, Targa M, Stefanelli A, Maniscalco P, Martini F, Tognon M, Borea PA: A_3 receptors are overexpressed in pleura from patients with mesothelioma and reduce cell growth via Akt/nuclear factor-κB pathway. Am J Respir Crit Care Med 2011;183:522-530.
18 Vanags DM, Pörn-Ares MI, Coppola S, Burgess DH, Orrenius S: Protease involvement in fodrin cleavage and phosphatidylserine exposure in apoptosis. J Biol Chem 1996;271:31075-31085.
19 Pietra G, Mortarini R, Parmiani G, Anichini A: Phases of apoptosis of melanoma cells, but not of normal melanocytes, differently affect maturation of myeloid dendritic cells. Cancer Res 2001;61:8218-8226.
20 Candé C, Cecconi F, Dessen P, Kroemer G: Apoptosis-inducing factor (AIF): key to the conserved caspase-independent pathways of cell death? J Cell Sci 2002;115:4727-4734.
21 Daugas E, Susin SA, Zamzami N, Ferri KF, Irinopoulou T, Larochette N, Prévost MC, Leber B, Andrews D, Penninger J, Kroemer G: Mitochondrio-nuclear translocation of AIF in apoptosis and necrosis. FASEB J 2000;14:729-739.
22 Ye H, Cande C, Stephanou NC, Jiang S, Gurbuxani S, Larochette N, Daugas E, Garrido C, Kroemer G, Wu H: DNA binding is required for the apoptogenic action of apoptosis inducing factor. Nat Struct Biol 2002;9:680-684.
23 Bilyy R, Kit Y, Hellman U, Stoika R: AMID: new insights on its intracellular localization and expression at apoptosis. Apoptosis 2008;13:729-732.

24 Li W, Sun L, Liang Q, Wang J, Mo W, Zhou B: Yeast AMID homologue Ndi1p displays respiration-restricted apoptotic activity and is involved in chronological aging. Mol Biol Cell 2006;17:1802-1811.
25 Marshall KR, Gong M, Wodke L, Lamb JH, Jones DJ, Farmer PB, Scrutton NS, Munro AW: The human apoptosis-inducing protein AMID is an oxidoreductase with a modified flavin cofactor and DNA binding activity. J Biol Chem 2005;280:30735-30740.
26 Ohiro Y, Garkavtsev I, Kobayashi S, Sreekumar KR, Nantz R, Higashikubo BT, Duffy SL, Higashikubo R, Usheva A, Gius D, Kley N, Horikoshi N: A novel p53-inducible apoptogenic gene, PRG3, encodes a homologue of the apoptosis-inducing factor (AIF). FEBS Lett 2002;524:163-171.
27 Varecha M, Amrichová J, Zimmermann M, Ulman V, Lukásová E, Kozubek M: Bioinformatic and image analyses of the cellular localization of the apoptotic proteins endonuclease G, AIF, and AMID during apoptosis in human cells. Apoptosis 2007;12:1155-1171.
28 Wu M, Xu LG, Li X, Zhai Z, Shu HB: AMID, an apoptosis-inducing factor-homologous mitochondrion-associated protein, induces caspase-independent apoptosis. J Biol Chem 2002;277:25617-25623.
29 Yaguchi T, Nakano T, Gotoh A, Nishizaki T: Adenosine promotes GATA-2-regulated p53 gene transcription to induce HepG2 cell apoptosis. Cell Physiol Biochem 2011;28:761-770.

Carcinogenesis vol.33 no.5 pp.969–975, 2012
doi:10.1093/carcin/bgs109
Advance Access publication February 21, 2012

Deficiency of Fyn protein is prerequisite for apoptosis induced by Src family kinase inhibitors in human mesothelioma cells

Ryoji Eguchi[1,2], Shuji Kubo[3], Hiromi Takeda[1], Toshiro Ohta[4], Chiharu Tabata[2], Hiroyasu Ogawa[1], Takashi Nakano[2] and Yoshihiro Fujimori[1,*]

[1]Laboratory of Cell Transplantation, Institute for Advanced Medical Sciences, [2]Department of Thoracic Oncology and [3]Department of Genetics, Hyogo College of Medicine, Nishinomiya, Hyogo 663-8501, Japan and [4]Department of Food and Nutritional Sciences, Graduate School of Nutritional and Environmental Sciences, University of Shizuoka, Shizuoka 422-8526, Japan

*To whom correspondence should be addressed. Tel/Fax: +81 798 45 6599; Email: fuji-y@hyo-med.ac.jp

Malignant mesothelioma is an aggressive tumor arising from mesothelial cells of serous membranes. Src family kinases (SFKs) have a pivotal role in cell adhesion, proliferation, survival and apoptosis. Here, we examined the effect of SFK inhibitors in NCI-H2052, ACC-MESO-4 and NCI-H28 cells, mesothelioma cell lines and Met5A, a human non-malignant mesothelial cell line. We found that PP2, a selective SFK inhibitor, inhibited SFK activity and induced apoptosis mediated by caspase-8 in NCI-H28 but not Met5A, NCI-H2052 and ACC-MESO-4 cells. Src, Yes, Fyn and Lyn protein, which are members of the SFK, were expressed in these cell lines, whereas NCI-H28 cells were deficient in Fyn protein. Small interfering RNA (siRNA) targeting Fyn facilitated PP2-induced apoptosis mediated by caspase-8 in NCI-H2052 and ACC-MESO-4 cells. PP2 reduced Lyn protein levels and suppressed SFK activity in all mesothelioma cell lines. Lyn siRNA induced caspase-8 activation and apoptosis in NCI-H28 cells but not in NCI-H2052 and ACC-MESO-4 cells. However, double RNA interference knockdown of Fyn and Lyn induced apoptosis accompanied by caspase-8 activation in NCI-H2052 and ACC-MESO-4 cells. Dasatinib, an inhibitor of multi-tyrosine kinases including SFK, also inhibited SFK activity and induced reduction of Lyn protein levels, caspase-8 activation and apoptosis in NCI-H28 cells but not in other cell lines. Present study suggests that SFK inhibitors induce caspase-8-dependent apoptosis caused by reduction of Lyn protein in Fyn-deficient mesothelioma cells.

Introduction

Malignant mesothelioma is an aggressive tumor arising from mesothelial cells of serous membranes, including pleura, peritoneum and pericardium (1–3). Mesothelioma is highly resistant to most chemotherapeutic agents (3), and radiation and surgical therapy generally show limited efficacy (3–5). New approaches for the treatment of malignant mesothelioma are urgently required.

Src family kinases (SFKs) are non-receptor and cytoplasmic tyrosine kinases that have a critical role in cell adhesion, proliferation, survival and apoptosis. In SFKs, Src, Yes and Fyn show ubiquitous expression, whereas others, including Lyn, exhibit more restricted tissue localization (6,7). SFK binds to focal adhesion kinase (FAK), a widely expressed cytoplasmic protein tyrosine kinase. Within SFK–FAK complex, SFK can trans-phosphorylate Tyr-576 and Tyr-577 in the kinase domain of FAK, which regulates migration, cell spreading and focal contact during cell motility (8,9).

In response to apoptotic stimuli, caspases relay messages through so-called initiator caspases to effector caspases (10). Dephosphorylation of Tyr-380, Tyr-397 and Tyr-465 in caspase-8, an initiator caspase, results in caspase-8 activation (11,12). Caspase cascade mediates apoptotic processes, such as externalization of phosphatidylserine, followed by cell death (10).

To explore a new therapeutic target against mesothelioma, we investigated the effects of SFK inhibitors, PP2 and dasatinib, on human mesothelioma cell lines, NCI-H2052, ACC-MESO-4 and NCI-H28 cells and a human non-malignant mesothelial cell line, Met5A. We found that SFK inhibitors induced apoptosis in NCI-H28 cells, which were deficient in Fyn protein. Further clarification of cell signaling pathways revealed that deficiency of Fyn protein is prerequisite for apoptosis induced by SFK inhibitors in human mesothelioma cells.

Abbreviations: FAK, focal adhesion kinase; GAPDH, glyceraldehyde-3-phosphate dehydrogenase; mRNA, messenger RNA; RNAi, RNA interference; SFK, Src family kinase; siRNA, small interfering RNA.

Materials and methods

Cell lines and culture

A non-malignant transformed human pleural mesothelial cell line, Met5A and two human mesothelioma cell lines, NCI-H2052 and NCI-H28, were obtained from the American Type Culture Collection (Rockville, MD). Another human mesothelioma cell line, ACC-MESO-4, was purchased from the RIKEN Bio-Research Center (Tsukuba, Japan). Cells were cultured as monolayers in RPMI-1640 medium (Sigma, St Louis, MO) with 10% fetal bovine serum (Sigma) at 37°C under a humidified atmosphere containing 5% CO_2.

Reagents and inhibitors

Antitumor agents and inhibitors were prepared in dimethyl sulfoxide using the following stock solutions: 10 mM PP2, 20 mM zIE(OMe)TD(OMe)-fmk, 40 mM zVAD(OMe)-fmk (BIOMOL, Plymouth Meeting, PA), 25 mM MG132 (BIOMOL) and 5 mM dasatinib (Biovision, Mountain View, CA). Dimethyl sulfoxide was used as a vehicle control as appropriate. All other chemicals were purchased from Sigma.

Treatment with antitumor agents and inhibitors

Cells were seeded as described below and cultured for 24 h. Old medium was aspirated, and fresh medium containing PP2 or dasatinib was added. For PP2 treatment, zVAD, MG132 or vehicle (dimethyl sulfoxide) was added to fresh medium containing PP2. Cells were then cultured for 3–72 h.

Cell viability analysis

Cells were seeded in a 96-well plate (Becton Dickinson Labware, Franklin Lakes, NJ) at 2×10^3 cells per well. Cell proliferation was determined by a colorimetric assay using Cell Counting Kit-8 (Dojin Chemical Institute, Kumamoto, Japan) according to the manufacturer's protocol. Color intensity was quantified as described earlier (13).

Western blotting and antibodies

Western blotting was performed as described earlier (13). Antibodies used to detect phospho-Src family (Tyr-416, #2101), phospho-FAK (Tyr-576/577, #3281), full-length and cleaved caspase-8 (#9746), caspase-3 (#9662), cleaved caspase-3 (#9661), Src (#2108) and phospho-Lyn (Tyr-507, #2731) were purchased from Cell Signaling Technology (Beverly, MA). Glyceraldehyde-3-phosphate dehydrogenase (GAPDH) antibody (#FL-335) was obtained from Santa Cruz Biotechnology (Santa Cruz, CA). FAK (#610087), Yes (#610375), Fyn (#610163) and Lyn antibody (#610003) were purchased from BD Biosciences (San Jose, CA). All western blot analyses were performed three times and the representative data are shown.

Flow cytometric analysis of apoptosis

Apoptosis was analyzed by flow cytometry using an Annexin V (Ax)-fluorescein isothiocyanate Kit (Medical & Biological Laboratories Co. Ltd, Nagoya, Japan) as described earlier (13). Briefly, 1×10^5 cells in a 60 mm dish (Becton Dickinson Labware) treated with PP2 or dasatinib were trypsinized, washed with phosphate-buffered saline and then labeled with Ax-fluorescein isothiocyanate and propidium iodide. Fluorescence intensity was measured using a Cytomics FC 500 flow cytometer and CXP software (Beckman Coulter, Fullerton, CA).

Quantitative reverse transcription–PCR analysis

Total RNA was isolated from cells using TRIzol reagent (Enzo Life Sciences, Farmingdale, NY). First-strand complementary DNA was synthesized from the

total RNA (1.25 μg) using the PrimeScript RT reagent kit (Takara Bio, Ohtsu, Japan) according to the manufacturer's instructions. PCR was performed on the synthesized complementary DNA product using TaqMan Gene Expression Master Mix (Applied Biosystems, Foster City, CA) according to the manufacturer's protocol. All reactions were carried out in triplicate. The sequences of the PCR primer pairs and fluorogenic probes used for Fyn and GAPDH are available on the Applied Biosystems website (http://www.appliedbiosystems.com/absite/us/en/home.html); Fyn assay ID: Hs00176628_m1; GAPDH assay ID: Hs99999905_m1). The amplification conditions were as follows: denaturation at 95°C for 15 s and annealing/extension at 60°C for 1 min for 60 cycles. The PCR products were analyzed using the ABI 7500 real-time PCR system (Applied Biosystems). Each messenger RNA (mRNA) level was normalized to the corresponding GAPDH mRNA level used as an internal control.

RNA interference

Small interfering RNAs (siRNAs) targeting Fyn [FYN Stealth Select RNA interference (RNAi) HSS103882], Yes (YES Stealth Select RNAi HSS187723) and Lyn (LYN Stealth Select RNAi HSS106213) and Stealth RNAi Negative Control Duplexes were purchased from Invitrogen (Carlsbad, CA). As control siRNA, #12935-146 (#146), #12935-115 (#115) and #12935-147 were used in NCI-H2052, ACC-MESO-4 and NCI-H28 cells, respectively. Stealth siRNA duplex oligoribonucleotides against Src (GenBank™ accession number NM_005417) were synthesized by Invitrogen. The sequences were as follows: sense 5′-CUGUGUUGUUGACAAUCUGGAGCCG-3′ and antisense 5′-CGGCUCCAGAUUGUCAACAACACAG-3′. The duplex oligoribonucleotides were dissolved in diethyl pyrocarbonate-treated water to make a 20 μM. Transient transfection of siRNAs was carried out using Lipofectamine RNAiMAX (Invitrogen) according to the manufacturer's instructions. Stealth RNAi compounds were used at a concentration of 10 nM in transfections as described earlier (13). Briefly, 2×10^5 cells were incubated in 10 ml of RPMI-1640 medium in a 100 mm dish overnight. Lipofectamine RNAiMAX and siRNA were each dissolved in 1 ml RPMI-1640 medium for 5 min at room temperature, combined and incubated for 15 min at room temperature to form complexes. Two milliliters of the mixture was added to the cell culture and incubated for 48 h. The cells were harvested by trypsinization and were seeded in a dish for PP2 treatment as described above.

Statistical analysis

All data are presented as the mean ± standard error of three independent experiments. Comparisons between two groups were performed using Student's unpaired *t*-test ($^*P < 0.05$, $^{**}P < 0.01$ and $^{***}P < 0.005$).

Results

PP2 induces apoptosis mediated by caspase-8 in NCI-H28 cells

We analyzed the effects of PP2, a selective SFK inhibitor, on mesothelioma cell lines (Figure 1). PP2 suppressed cell viability of all mesothelioma cell lines used more markedly than that of Met5A cells in a concentration-dependent manner (Figure 1A). We used an antibody recognizing phosphorylation of tyrosine residue corresponding to Tyr-416 of Src in various SFKs (Figure 1B). PP2 inhibited the phosphorylation of SFK (lower two arrows in Figure 1B) and that of p-FAK in a concentration-dependent manner in all mesothelioma cell lines used. These results show that enzyme activity of SFK is suppressed by PP2. Intriguingly, PP2 significantly induced apoptosis in NCI-H28 cells (Figure 1C). In NCI-H28 cells, PP2 also induced cleavage of caspase-8 and caspase-3 in a time-dependent manner (Figure 1D). Furthermore, PP2-induced apoptosis in NCI-H28 cells

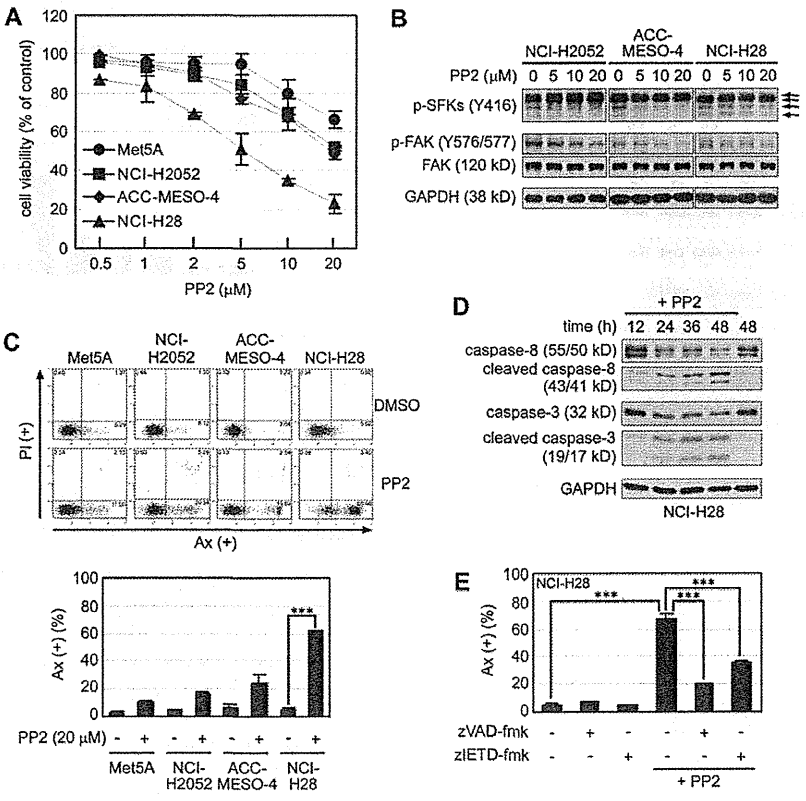

Fig. 1. PP2 induces apoptosis mediated by caspase-8 in NCI-H28 cells. (**A**) PP2 suppresses cell viability of NCI-H2052, ACC-MESO-4 and NCI-H28 cells more markedly than that of Met5A cells. These cell lines were treated with PP2 for 48 h at the indicated concentrations. Cell viability was assessed using the Cell Counting Kit-8 assay. (**B**) PP2 suppresses enzyme activity of SFK. Cell extracts were prepared from NCI-H2052, ACC-MESO-4 and NCI-H28 cells treated with 5–20 μM PP2 for 6 h as described in Materials and methods. Arrows indicate phosphorylation of Tyr-416 in various SFKs. (**C**) PP2 induces apoptosis in NCI-H28 cells, but not in Met5A, NCI-H2052 and ACC-MESO-4 cells. The numbers of (Ax+) apoptotic cells were markedly increased 72 h after the treatment with 20 μM PP2 in NCI-H28 cells but not in other cell lines. (**D**) PP2 induces activation of caspase-8 and caspase-3. Cell extracts were prepared from NCI-H28 cells treated with 20 μM PP2 for 12–48 h. (**E**) PP2-induced apoptosis in NCI-H28 cells is suppressed by zVAD-fmk and zIETD-fmk. NCI-H28 cells were treated with 20 μM PP2 alone or together with 100 μM zVAD-fmk and 50 μM zIETD-fmk for 72 h and analyzed for Ax(+) apoptotic cells by flow cytometry.

was significantly suppressed by zVAD-fmk, a broad-spectrum caspase inhibitor, and zIETD-fmk, a specific caspase-8 inhibitor (Figure 1E). These results suggest that PP2 suppresses SFK activity and induces apoptosis mediated by caspase-8 in NCI-H28 cells.

Deficiency of Fyn protein is caused by transcriptional repression of Fyn mRNA in NCI-H28 cells, and Lyn is expressed in mesothelial and mesothelioma cells

We examined whether SFK expression is involved in PP2-induced apoptosis in mesothelioma cells (Figure 2). Src, Yes and Lyn protein were detected in all cell lines used, but NCI-H28 cells were deficient in Fyn protein, whereas it was expressed in other three cell lines (Figure 2A). Phosphorylation of SFK in NCI-H2052 and ACC-MESO-4 but not NCI-H28 cells was higher than that in Met5A cells. We then examined expression of Fyn mRNA using quantitative reverse transcription–PCR (Figure 2B). It was found that Fyn mRNA expression in NCI-H28 cells was much lower than that in other cell lines used. Additional experiments using other PCR primer pairs and fluorogenic probes also showed that Fyn mRNA was not completely absent in NCI-H28 cells (data not shown). These results suggest that deficiency of Fyn protein is caused by transcriptional repression of Fyn mRNA in NCI-H28 cells and that Lyn is expressed in mesothelial and mesothelioma cells.

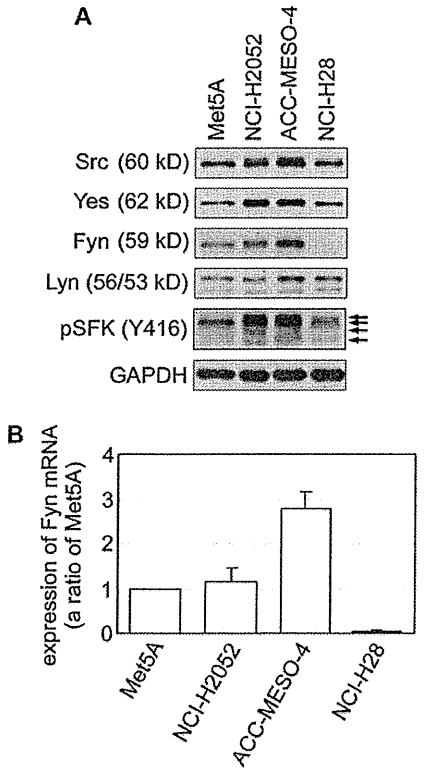

Fig. 2. Deficiency of Fyn protein is caused by transcriptional repression of Fyn mRNA in NCI-H28 cells. (**A**) Expression and phosphorylation of SFK in Met5A, NCI-H2052 and ACC-MESO-4 and NCI-H28 cells. Cell extracts were prepared from these cell lines incubated for 72 h. (**B**) Fyn synthesis is suppressed by transcriptional repression of Fyn mRNA in NCI-H28 cells. Total RNA was isolated from these cells after incubation for 72 h as described in Materials and methods.

Fyn-knockdown facilitates PP2-induced apoptosis in mesothelioma cells

To further investigate whether transcriptional repression of Fyn mRNA is related to PP2-induced apoptosis, we performed RNAi using siRNA targeting Fyn in NCI-H2052 and ACC-MESO-4 cells (Figure 3). Fyn siRNA abrogated expression of Fyn protein with no effect on expression of Src, Yes and Lyn protein (Figure 3A). In NCI-H2052 and ACC-MESO-4 cells treated with Fyn siRNA, PP2 induced apoptosis more significantly than in these cells treated with control siRNA (Figure 3B). Furthermore, PP2 induced cleavage of caspase-8 and caspase-3 in these Fyn-knockdown mesothelioma cell lines (Figure 3C). These results suggest that Fyn-knockdown facilitates PP2-induced apoptosis in Fyn-expressing mesothelioma cells.

SFK inhibition induces apoptosis in Fyn-deficient mesothelioma cells

We then analyzed whether PP2-induced apoptosis is related to SFK inhibition in NCI-H28 cells (Figure 4). Western blot analysis showed that PP2 suppressed phosphorylation of Tyr-416 in SFKs and that of

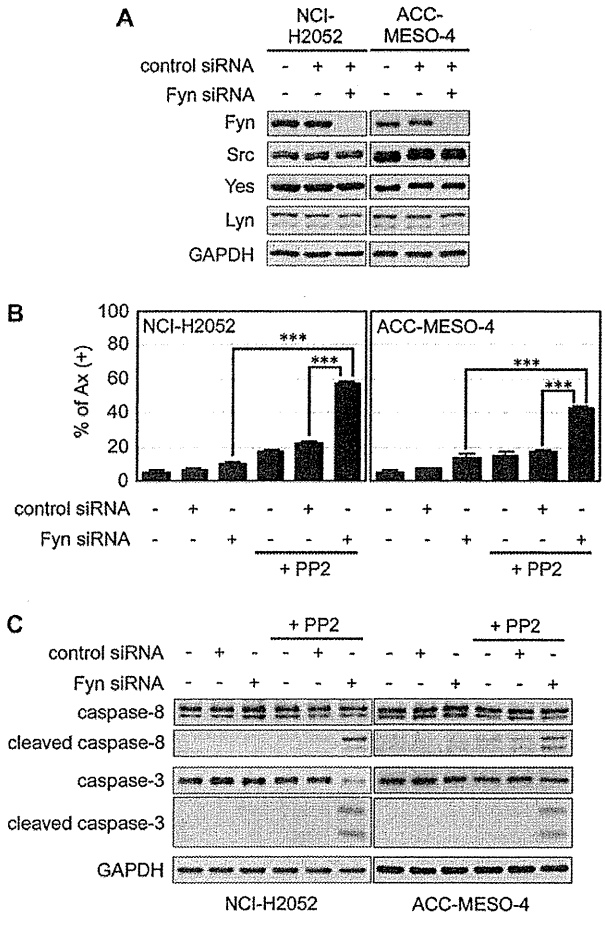

Fig. 3. Fyn-knockdown facilitates PP2-induced apoptosis in mesothelioma cells. (**A**) Fyn-knockdown in mesothelioma cells. NCI-H2052 and ACC-MESO-4 cells were transfected with 10 nM siRNA against Fyn mRNA or 10 nM control siRNA for 48 h, harvested by trypsinization and incubated for 24 h. Cell extracts were prepared from NCI-H2052 and ACC-MESO-4 cells after the incubation for 24 h. (**B**) Fyn-knockdown facilitates PP2-induced apoptosis in mesothelioma cells. NCI-H2052 and ACC-MESO-4 cells, transfected with Fyn and control siRNAs, were treated with 20 μM PP2 for 72 h and analyzed for Ax (+) apoptotic cells by flow cytometry. (**C**) PP2 induces activation of caspase-8 and caspase-3 in Fyn-knockdown mesothelioma cells. NCI-H2052 and ACC-MESO-4 cells, transfected with Fyn and control siRNA, were treated with 20 μM PP2 for 48 h.

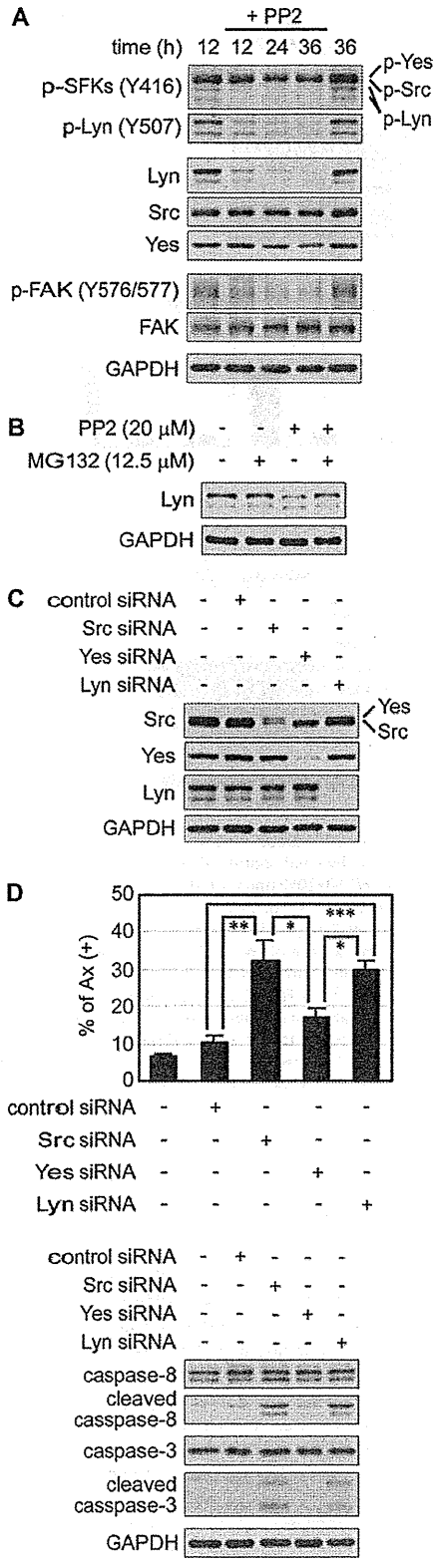

Fig. 4. Src and Lyn suppress apoptosis accompanied by caspase-8 activation in Fyn-deficient mesothelioma cells. (**A**) PP2 inhibits SFK activity and reduces Lyn protein levels. Cell extracts were prepared from NCI-H28 cells treated with 20 μM PP2 for 12–36 h. (**B**) Lyn protein is degraded by the ubiquitin-proteasome pathway. Cell extracts were prepared from NCI-H28 cells treated with 20 μM PP2 together with 12.5 μM MG132 for 12 h. (**C**) Knockdown of Src, Yes and Lyn in NCI-H28 cells. The cells were transfected with Src, Yes and Lyn siRNAs and control siRNA for 48 h, harvested by trypsinization and incubated for 24 h, and cell extracts were prepared as described in Materials and methods. (**D**) Src and Lyn siRNAs, but not Yes siRNA, significantly induce apoptosis accompanied by caspase-8 activation in NCI-H28 cells. The cells were transfected with Src, Yes and Lyn siRNAs and control siRNA for 48 h, harvested by trypsinization and incubated for 24 h. The old medium was exchanged after the incubation for 24 h, and the cells were incubated further for 72 h and analyzed for Ax (+) apoptotic cells by flow cytometry. For western blotting, cell extracts were prepared from NCI-H28 cells incubated for 72 h after the medium exchange.

Tyr-507 in Lyn (Figure 4A). PP2 also induced reduction of Lyn protein levels but not Src or Yes protein levels. These results suggest that PP2-inhibited Lyn phosphorylation is caused by reduction of Lyn protein. Lyn protein has been reported to be degraded by the ubiquitin-proteasome pathway (14). Therefore, we examined the involvement of this pathway. MG132, a proteasome inhibitor, suppressed PP2-induced reduction of Lyn protein (Figure 4B), suggesting that Lyn protein is degraded by the ubiquitin-proteasome pathway. To investigate which SFKs are involved in apoptosis mediated by caspase-8 in Fyn-deficient mesothelioma cells, we analyzed the induction of apoptosis in NCI-H28 cells treated with siRNAs targeting Src, Yes and Lyn. Each siRNA abrogated expression of respective SFK protein (Figure 4C). Src and Lyn siRNAs, but not Yes siRNA, significantly induced apoptosis in NCI-H28 cells (Figure 4D). In addition, knockdown of Src and Lyn, but not of Yes, induced cleavage of caspase-8 and caspase-3. These results suggest that Src and Lyn suppress caspase-8 activation and apoptosis in Fyn-deficient mesothelioma cells.

Both Fyn and Lyn suppress apoptosis in mesothelioma cells

We analyzed whether Src, Yes and Lyn are involved in apoptosis in Fyn-expressing mesothelioma cells (Figure 5). In NCI-H2052 and ACC-MESO-4 cells treated with Fyn siRNA and control siRNA, PP2 suppressed FAK phosphorylation and reduced Lyn protein levels (Figure 5A), whereas PP2 failed to induce caspase-8 cleavage and apoptosis in these cells treated with control siRNA (Figure 3B and C). We then investigated apoptotic induction by RNAi knockdown of Src, Yes and Lyn in Fyn-expressing mesothelioma cells. Individual siRNAs abrogated expression of respective SFK protein but failed to induce apoptosis in NCI-H2052 and ACC-MESO-4 cells (Figure 5B). We further performed knockdown of both Fyn and Lyn. The double knockdown of Fyn and Lyn efficiently abrogated expression of both Fyn and Lyn with no effect on expression of Src and Yes protein (Figure 5C). The double knockdown induced significant apoptosis and cleavage of caspase-8 and caspase-3 in NCI-H2052 and ACC-MESO-4 cells (Figure 5D). Collectively, these results show that PP2-induced apoptosis is caused by reduction of Lyn protein in Fyn-deficient mesothelioma cells.

SFK inhibitors induce reduction of Lyn protein followed by caspase-8-dependent apoptosis in Fyn-deficient mesothelioma cells

To further investigate whether other SFK inhibitors are able to induce apoptosis in Fyn-deficient mesothelioma cells, we treated these cell lines with dasatinib, an inhibitor of multi-tyrosine kinase including Bcr-Abl kinase and SFK (Figure 6). Dasatinib suppressed cell viability of all MM cell lines used more markedly than that of Met5A cells in a concentration-dependent manner (Figure 6A). In addtion, Dasatinib significantly induced apoptosis in NCI-H28 cells but not other mesothelioma cell lines (Figure 6B). Dasatinib inhibited phosphorylation of SFKs and FAK, reduced Lyn protein, but not of Src and Yes protein levels and cleavage of caspase-8 and caspase-3 in a concentration- and time-dependent manner in NCI-H28 cells (Figure 6C). Dasatinib also induced reduction of Lyn protein levels in NCI-H2052 and ACC-MESO-4 cells (data not shown) but failed to induce cell death in these Fyn-expressing mesothelioma cell lines

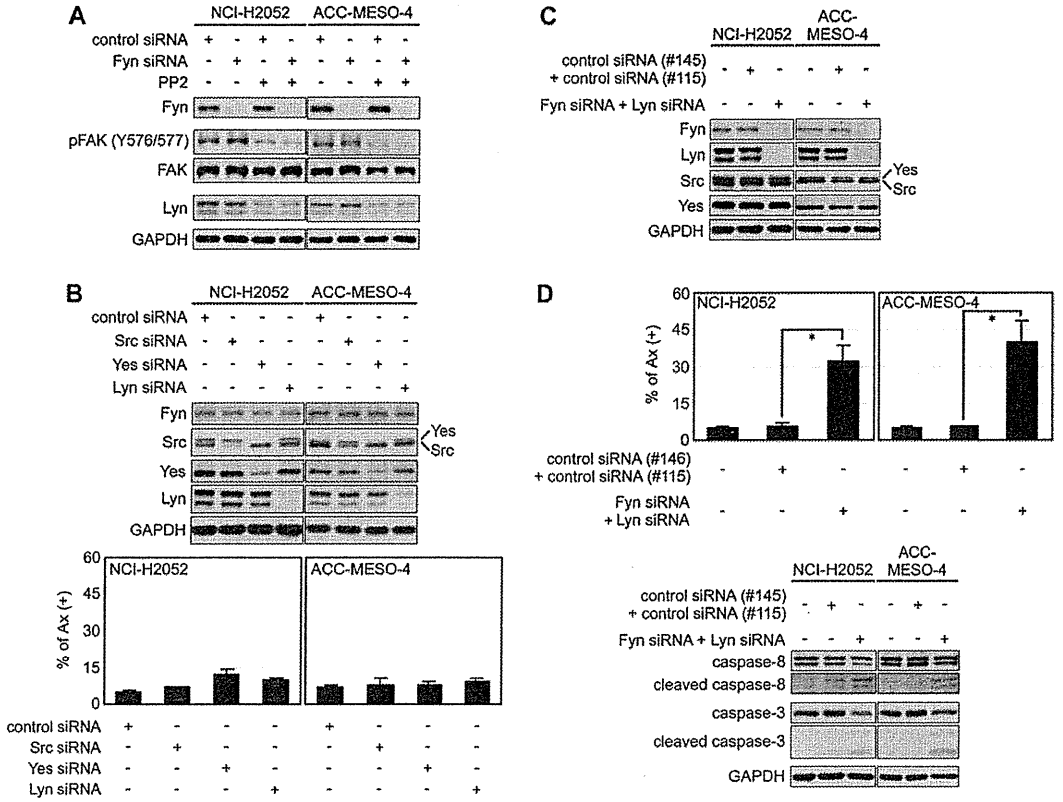

Fig. 5. Both Fyn and Lyn suppress apoptosis accompanied by caspase-8 activation in mesothelioma cells. (**A**) PP2 inhibits SFK activity and reduces Lyn protein levels without Fyn-knockdown in mesothelioma cells. NCI-H2052 and ACC-MESO-4 cells, transfected with Fyn and control siRNAs, were treated with 20 μM PP2 for 24 h. (**B**) siRNA of individual SFK fails to induce apoptosis in Fyn-expressing mesothelioma cells. NCI-H2052 and ACC-MESO-4 cells were transfected with Src, Yes and Lyn siRNAs and control siRNA for 48 h, harvested by trypsinization and further incubated at 37°C for 24 h. For western blotting, cell extracts were prepared from NCI-H2052 and ACC-MESO-4 cells after the incubation for 24 h. The old medium was exchanged after the incubation for 24 h, and the cells were incubated further for 72 h and analyzed for Ax (+) apoptotic cells by flow cytometry. (**C**) Double knockdown of Fyn and Lyn in Fyn-expressing mesothelioma cells. NCI-H2052 and ACC-MESO-4 cells were transfected with both Fyn and Lyn siRNAs or both control siRNA (#146) and control siRNA (#115) for 48 h. The cells were harvested by trypsinization and incubated for 24 h. Cell extracts were prepared from NCI-H2052 and ACC-MESO-4 cells after the incubation for 24 h. (**D**) Double knockdown of Fyn and Lyn induces apoptosis accompanied by caspase-8 activation in mesothelioma cells. NCI-H2052 and ACC-MESO-4 cells were transfected with both Fyn and Lyn siRNAs or both control siRNA (#146) and control siRNA (#115) for 48 h, and the cells were harvested by trypsinization and further incubated at 37°C for 24 h. The old medium was exchanged after the incubation for 24 h. The cells were incubated further for 72 h and analyzed for Ax (+) apoptotic cells by flow cytometry. For western blotting, cell extracts were prepared from NCI-H2052 and ACC-MESO-4 cells incubated for 72 h after the medium exchange.

(Figure 6B). These results suggest that dasatinib, like PP2, is able to induce caspase-8-dependent apoptosis mediated by reduction of Lyn protein in Fyn-deficient mesothelioma cells.

Discussion

Malignant mesothelioma is refractory to conventional chemotherapy, which is related to the resistance to induction of apoptosis by chemotherapeutic agents (3). PP2 has been shown to induce apoptosis in some tumor cells, including B-cell leukemia and breast cancer and hepatoma but not in primary hepatocytes (15–17). In the present study, we found that PP2 induced apoptosis mediated by caspase-8 in a mesothelioma cell line, NCI-H28, but not a non-malignant mesothelioal cell line, Met5A (Figure 1).

Fyn is generally expressed in various tissues (7). Fyn has been recognized as an important mediator of cell cycle, growth, survival and cell–cell adhesion (18). Western blot and quantitative reverse transcription–PCR analyses revealed that Fyn protein is detected in all cell lines used except NCI-H28 cells, and Fyn synthesis is suppressed by transcriptional repression of Fyn mRNA in NCI-H28 cells (Figure 2). In prostate cancer, Fyn is reported to be downregulated by both chromosomal deletion and promoter hypermethylation (19). However, Fyn promoter regions were not methylated in NCI-H28 cells (data not shown). Detailed investigation to clarify how transcription of Fyn mRNA is repressed in NCI-H28 cells is needed. We also found that Fyn-knockdown facilitated PP2-induced apoptosis in mesothelioma cells (Figure 3). Furthermore, we observed that Fyn-expressing mesothelioma cells were resistant to apoptosis induced by SFK inhibition and knockdown of individual SFK (Figures 3 and 5). Fyn is overexpressed in various cancers, including glioblastoma, squamous cell carcinoma, melamona and chronic myeloid leukemia (18,20). In addition, chronic myeloid leukemia cells overexpressing Fyn have been shown to be resistant to PD166326, a Bcr-Abl kinase and SFK inhibitor (21). We found that Fyn-knockdown or deficiency of Fyn protein is insufficient to induce apoptosis but facilitated PP2-induced apoptosis in mesothelioma cells (Figures 1–3).

Lyn is known to be expressed in all blood cells except T lymphocytes (22). In neutrophils, PP2 is reported to reduce Lyn protein levels and apoptosis accompanied by caspase-8 activation (12). Our results revealed that Lyn is expressed in mesothelial and mesothelioma cells and degraded by the ubiquitin-proteasome pathway in mesothelioma cells (Figures 2 and 4). In addition, Lyn-knockdown induced apoptosis accompanied by caspase-8 activation in NCI-H28 cells (Figure 4). However, PP2-induced reduction of Lyn protein levels